Journal of Hydrology (2007) 344, 146–156

available at www.sciencedirect.com

ScienceDirect

journal homepage: www.elsevier.com/locate/jhydrol

Annual groundwater evapotranspiration mapped from single satellite scenes

David P. Groeneveld [a,*], William M. Baugh [a], John S. Sanderson [b], David J. Cooper [c]

[a] HydroBio, Advanced Remote Sensing, Santa Fe, NM 87501, USA
[b] Department of Biology, Colorado State University, Fort Collins, CO 80523, USA
[c] Department of Forest, Rangeland and Watershed Stewardship, Colorado State University, Fort Collins, CO 80523, USA

Received 2 August 2006; received in revised form 9 July 2007; accepted 10 July 2007

KEYWORDS
NDVI*;
Phreatophyte;
Basin water balance;
Remote sensing;
ET mapping;
San Luis Valley

Summary Evapotranspiration (ET) data measured using micrometeorological equipment were obtained from three separate studies conducted in arid and semi-arid shallow groundwater environments in California, New Mexico and Colorado. These locations have great diversity in (1) climate expression: monsoon versus Mediterranean annual precipitation patterns and comparatively long versus short growing seasons; and in (2) vegetation cover: alkali scrub, shallow groundwater meadows, and monocultures of saltcedar and cottonwood. Actual ET (ET_a), measured from 24 site- and year-combinations was paired with NDVI*, a derivation of normalized difference vegetation index. NDVI* was extracted from corresponding locations in nine mid-summer Landsat TM5 and TM7 scenes during 1999–2002, with single mid-summer scenes used for estimation of annual total ET_a. NDVI* was a competent estimator of a derivation of ET, ET*, calculated by subtracting annualized precipitation and normalizing by an annualized reference ET, (ET_0). This relationship was used to estimate annual total ET_a, derived solely from remote sensing and weather data. Residual error decreased as ET_a increased with well-balanced data scatter indicating lack of systematic error. These results demonstrate a simple and robust method that can be used to map annual ET as a first-order approximation from a single mid-summer satellite scene for any arid or semi-arid shallow groundwater environment where sufficient weather data exist for calculating annual precipitation and reference ET.

Introduction

Quantification of the water balance of arid and semi-arid groundwater basins can be used to define safe yield for local

* Corresponding author. Tel.: +1 505 992 0234; fax: +1 505 992 0274.
E-mail address: david@hydrobio.org (D.P. Groeneveld).

0022-1694/$ - see front matter © 2007 Elsevier B.V. All rights reserved.
doi:10.1016/j.jhydrol.2007.07.002

use and export. Evapotranspiration (ET) discharge from groundwater is often a dominant component of outflow from these basins and, therefore, requires accurate spatial quantification. In many groundwater basins across the Basin and Range Province of western North American, large valley-floor regions underlain by shallow groundwater support a vegetation cover of phreatophytes (plants that use shallow groundwater: Meinzer, 1927). This plant cover may account for the majority of a basin's ET (Nichols et al., 1997; Nichols, 2000). Broadband data sensed by Landsat Thematic Mapper (TM) satellite or its equivalent, may offer practical approaches for ET estimation for groundwater basins that can encompass thousands of square miles. Calibration using sites with known ET is always recommended, however, *a-priori*, sites where ET was measured for a season or more, and hence suitable for calibration, are usually lacking. Recognizing this limitation, this paper presents methods for mapping ET as a first-order approximation without the requirement of a calibration data set.

Groeneveld and Baugh (2007) evaluated a derivation of NDVI to eliminate non-systematic variation, NDVI*, that stretches the NDVI distribution for vegetation from zero to one. In this paper, the vegetation signature provided by NDVI* is calibrated to map total annual actual ET (ET_a). The calibration requires only sufficient weather data to calculate total annual actual ET_0, a grass reference ET, calculated by the Penman-Monteith equation as described by Allen et al. (1998) in the methods collectively known as FAO-56. Since NDVI* is a scalar value for multiplication by ET_0, it is functionally the same as a crop coefficient (K_c, Allen et al., 1998).

Theory supporting prediction of annual ET using peak season NDVI*

NDVI utilizes the great difference in two adjacent bands in the red and near-infrared portion of the spectrum that occurs when viewing healthy vegetation. Chlorophyll, responsible for the green color of plants, absorbs red light while leaf tissue is highly reflective in the near infrared (Buschmann and Nagel, 1993). NDVI is calculated by subtracting the response in the red band (TM Band 3) from the reflectance in the near-infrared band (NIR; TM Band 4) and then dividing the sum of the reflectances for these two bands (Rouse et al., 1974). Chlorophyll is a physiologically expensive molecule for plants to produce, and so, the amount of chlorophyll relates directly to the rate of photosynthesis (Tucker and Sellers, 1986; Sellers et al., 1992). Photosynthesis requires leaf conductance for the uptake of carbon dioxide, and during this process water is evaporated to the atmosphere. Because of this chain of related properties, NDVI can be used as a competent surrogate for estimation of both photosynthetic activity (Sellers et al., 1992; Chong et al., 1993); and ET (Kerr et al., 1989; Chong et al., 1993; Kustas et al., 1994; Seevers and Ottmann, 1994; Szilagyi et al., 1998; Szilagyi, 2000, 2002). As shown by Baugh and Groeneveld (2006) and Groeneveld and Baugh (2007), NDVI provides greatly improved prediction after conversion to NDVI*, a process that removes non-systematic variation.

Dry climate, vegetated, shallow groundwater environments offer the potential to use simplified relationship for satellite-based ET mapping using NDVI. Annual ET on such sites is buffered from wide inter-annual swings by the presence of shallow groundwater or water retained within the soil column, in the event of inter-annual water table fluctuation. Under these conditions, the meager precipitation tends to be a relatively small component of ET_a and thus, interception losses and soil evaporation will tend to be small proportions of the water balance. Because groundwater provides a stable supply, ET_a will tend to track reference ET (ET_0) a measure of the evaporating power of the atmosphere, dependent upon air temperature, humidity and wind speed (Allen et al., 1998) as moderated by the plant canopy. Solar radiation provides the energy to drive this process and in such ideal environments, both ET_a and ET_0 will tend to rise and fall in an orderly manner with the annual curves of daily solar radiation. Likewise, the leaf area of vegetation canopies in temperate climates rises to a maximum during mid growing season and then falls off to wintertime senescence (Or and Groeneveld, 1994). Inherent in the assumption for an ET mapping routine based on NDVI, is that higher canopy expression, for example leaf area index, equates to higher levels of NDVI expressed in satellite data. This relationship has been well documented in the literature (e.g., Curran et al., 1992; Hobbs, 1995; Grist et al., 1997; Paruelo et al., 1997).

Methods

Three existing data sets that contained sufficient daily ET measurements to calculate total water-year ET_a were chosen for study. These data are from three widely separate environments, each with arid climates underlain by shallow groundwater: a shallow groundwater meadow and alkali scrub in the San Luis Valley, Colorado; alkali scrub in San Luis Valley and Owens Valley, California; and salt cedar and cottonwood adjacent to the Rio Grande in the Bosque del Apache, New Mexico (Fig. 1). Species and site information are listed in Table 1. The three ET studies provided annual or, quasi-annual records of ET_a using *in situ* micrometeorological equipment. Global positioning system measurements for these sites permitted locating each study site on satellite imagery for extraction and comparison of NDVI.

Remote sensing data

The methods described in Groeneveld and Baugh (2007) were used to process nine mid-summer TM scenes selected from the Landsat archives. Each scene was georeferenced to one pixel, or better, accuracy using road intersections and other features on USGS 1:100,000 scale Digital Line Graph maps, and then processed to reflectance using gains, offsets, and ephemeris data contained in the header files accompanying the imagery data (Irish, 1999). Reflectance data for all pixels were atmospherically corrected by dark object subtraction based on TM Band 3 where the NIR Band 4 = 0.792 of Band 3, a method that was also used in Baugh and Groeneveld (2006) and Groeneveld and Baugh (2007).

Data for each site were then extracted from the geo- and atmospherically corrected scenes using 3×3 pixel matrices

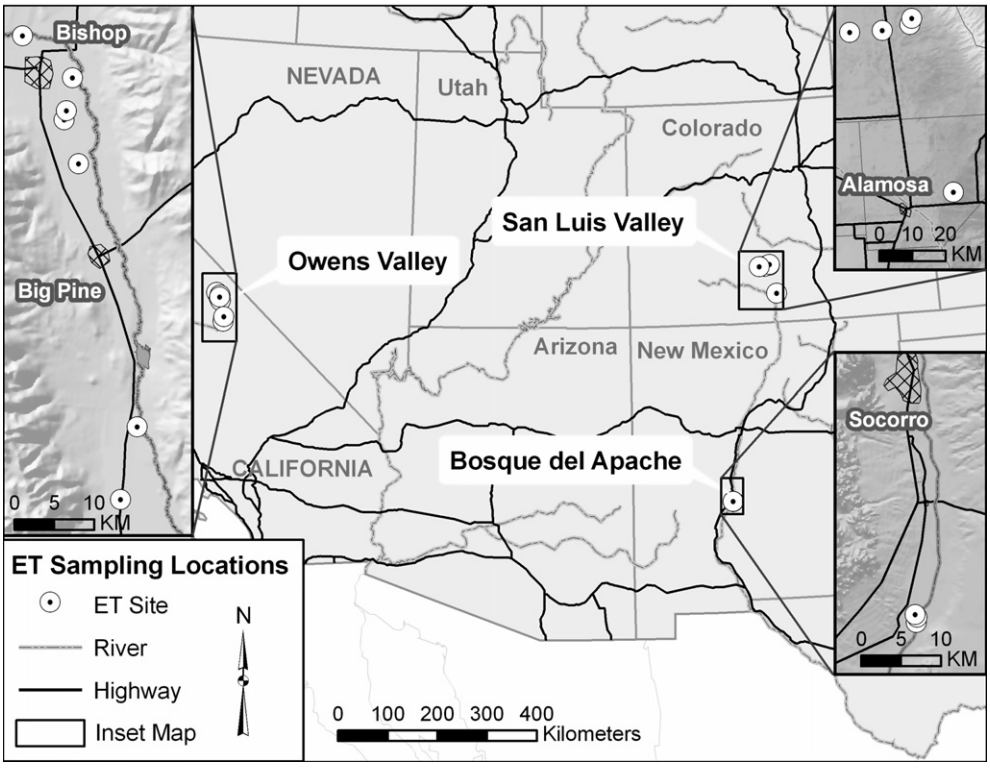

Figure 1 Location maps of sample locations.

Table 1 ET data collection sites — years operated, plant species and depth to water

	Year	Site	Dominant species	Depth to water (m)
Owens Valley, California	2000	BLK100	Saltgrass, alkali sacaton	2.0—2.5
	2001	BLK100	Saltgrass, alkali sacaton	2.2—2.3
	2001	BLK009	Salt rabbitbrush, alkali sacaton	2.6—3.2
	2001	PLC045	Nevada saltbush	3.8—4.1 (est.)
	2002	BLK100	Saltgrass, alkali sacaton	2.3—3.2
	2002	FSL138	Saltgrass, basin wildreye, alkali sacaton	1.2—2.1
	2002	PLC018	Salt rabbitbrush	>5.0
	2002	PLC074	Greasewood, Nevada saltbush, saltgrass	2.1—2.4
	2002	PLC185	Greasewood	>4.0
			(*Source:* Harrington et al., 2003)	
San Luis Valley, Colorado	2000	Stannard	Greasewood, salt rabbitbrush	3.1—3.5
	2002	Crestone	Greasewood, salt rabbitbrush, saltgrass	1.0—1.4
	2002	Moffat	Greasewood, salt rabbitbrush, alkali sacaton, saltgrass	1.2—1.5
	2002	Rito Alto	Grass/grasslike:bluegrass, redtop, sedges, walking sedge	<1.0 (est.)
	2002	Thicket	Greasewood, salt rabbitbrush	1.0—1.2
			(*Source:* Cooper et al., 2004)	
Bosque del Apache, New Mexico	1999	SSCT	Saltcedar	
	1999	NSCT	Saltcedar	0.5—2.0 (a)
	1999	SCWT	Cottonwood	2.0—2.8 (a)
	2000	SSCT	Saltcedar	3.0—3.6
	2000	NSCT	Saltcedar	2.7—3.2
	2001	SSCT	Saltcedar	NA
	2001	NSCT	Saltcedar	NA
	2002	SSCT	Saltcedar	NA
	2002	NSCT	Saltcedar	NA
	2002	SCWT	Cottonwood	NA
			Source: http:/tamarisk.nmsu.edu, Bawazir, 2000	

(85.5 m × 85.5 m) that were roughly coincident with the area measured for ET. These data were averaged to provide a more robust area-wide measure of NDVI.

As described in Groeneveld and Baugh (2007), NDVI* is stretched to cover the distribution from 0 to 1 in a process that removes variation inherent in NDVI data sets thought to be due to atmospheric, soil and vegetation factors (Huete and Liu, 1994; Liu and Huete, 1995). NDVI* uses two parameters $NDVI_0$ and $NDVI_S$ (values listed in Table 2) that represent NDVI at zero vegetation cover and at saturation (Gillies et al., 1997).

$$NDVI^* = (NDVI - NDVI_0)/(NDVI_S - NDVI_0) \quad (1)$$

NDVI*, thus, enables comparison of NDVI measured at different locations or, as discussed by Groeneveld and Baugh (2007), with different sensors, and at different times with correspondingly different atmospheric opacities. Conversion from NDVI to NDVI* removes such non-systematic variability and improves both accuracy and precision of the vegetation-based predictions it affords.

Similar to the calculation of NDVI*, ET was transformed into ET* according to Eq. (2).

$$ET^* = (ET_a - \text{Precipitation})/(ET_0 - \text{Precipitation}) \quad (2)$$

where ET_a is actual ET, ET_0 is grass reference ET and all components are annual totals.

ET data and weather

Micrometeorological measurement of ET is equipment intensive, expensive, and time consuming. Micrometeorologic data are included here but only with brief description of the methods taken directly from the text of each cited source. All ET data presented in this paper are annual water-year totals, for measurements taken, or projected, for the period October 1 through September 30. These data were collected at three locations, Owens Valley, California, San Luis Valley, Colorado, and Bosque del Apache, New Mexico (Fig. 1).

Owens Valley, California

Harrington et al. (2003) used three-dimensional eddy covariance (EC), a measure of the turbulent fluxes of water vapor (Arya, 2001) to measure the ET of alkali scrub sites on the floor of Owens Valley, California. These measurements were obtained using the equipment described in Table 3. Sites were chosen for homogeneous vegetation within the fetch influence as calculated by methods keyed to the height and roughness of the vegetation (Gash, 1986). As an independent check of ET measured by EC, each site was also outfitted with net radiometers and soil heat flux plates in order to calculate ET independently using the energy balance approach. Two corrections for sensor bias

Table 2 NDVI and NDVI* calculated from nine TM images for each of the 24 site/year combinations ($n = 24$)

	Year	TM overpass date	3 × 3 average	Stretch parameters (intercepts)		NDVI*
			$NDVI_{raw}$	$NDVI_0$	$NDVI_s$	
Owens Valley, California						
BLK100	2000	4-July	0.2247	0.0706	0.8995	*0.1859*
BLK100	2001	23-July	0.2932	0.0660	0.9119	*0.2686*
BLK009	2001	23-July	0.2348	0.0660	0.9119	*0.1995*
PLC045	2001	23-July	0.1634	0.0660	0.9119	*0.1151*
BLK100	2002	10-July	0.2567	0.0627	0.9113	*0.2286*
FSL138	2002	10-July	0.3565	0.0627	0.9113	*0.3462*
PLC018	2002	10-July	0.1138	0.0627	0.9113	*0.0601*
PLC074	2002	10-July	0.1832	0.0627	0.9113	*0.1420*
PLC185	2002	10-July	0.1049	0.0627	0.9113	*0.0497*
San Luis Valley, Colorado						
Standard	2000	19-July	0.1591	0.1047	0.8995	*0.0685*
Crestone	2002	10-August	0.2122	0.0965	0.9640	*0.1334*
Moffat	2002	10-August	0.1833	0.0965	0.9640	*0.1000*
Rito Alto	2002	10-August	0.5974	0.0965	0.9640	*0.5773*
Thicket	2002	10-August	0.3768	0.0965	0.9640	*0.3231*
Bosque del Apache New Mexico						
SSCT	1999	1-July	0.7360	0.0959	0.9344	*0.7634*
NSCT	1999	1-July	0.7071	0.0959	0.9344	*0.7289*
SCWT	1999	1-July	0.4009	0.0959	0.9344	*0.3637*
SSCT	2000	19-July	0.7588	0.0918	0.9263	*0.7993*
NSCT	2000	19-July	0.7466	0.0918	0.9263	*0.7846*
SSCT	2001	29-June	0.7464	0.0836	0.9104	*0.8016*
NSCT	2001	29-June	0.6865	0.0836	0.9104	*0.7292*
SSCT	2002	2-July	0.6571	0.1631	0.9393	*0.6365*
NSCT	2002	2-July	0.6447	0.1631	0.9393	*0.6204*
SCWT	2002	2-July	0.4736	0.1631	0.9393	*0.4001*

Table 3 Equipment lists as described by each study's authors

Owens Valley, California	Harrington et al. (2003)
ET by Eddy Covariance Method	Equipment per Campbell Scientific
Windspeed	CSAT sonic anemometer
Water vapor density	KH20 krypton hygrometer
Air temperature	Fine-wire thermocouple, 2.5 above ground
Sensor systems were deployed 2.5 m above ground	
San Luis Valley, Colorado	(Cooper et al., 2006)
ET Bowen Ratio Method	Equipment per REBS, Inc.
Humidity	Hygroscopic polymer capacitance chip
Temperature	Platinum resistance elements
Humidity and temperature sensing separated 1.0 m vertically, switched/15 minutes	
Net radiation	REBS, Inc. Q*7.1 Net Radiometer, 2.5 m above ground
Soil heat flux	Heat flow transducers and buried probes in top 5 cm of soil
Sensor systems were deployed 2.5 m above ground	
Bosque del Apache, New Mexico	Bawazir (2000)
ET by Eddy Covariance Method equipment per Campbell Scientific	12.5 m towers in salt cedar, 15 m tower in Cottonwood
Windspeed	CSAT3 sonic anemometer
Water vapor density	KH2O krypton hygrometer
Air temperature	FW05 fine-wire thermocouple (12.7 μm)
Relative humidity/temperature	HMP45C sensor
ET by OPEC method	
Vertical flux	R.M. Young Company Model 27106Gill propeller anemometer
Temperature	76 μm diameter type E fine-wire thermocouple
Propeller and thermocouple at 6.8 m above 6-m tall salt cedar canopy and 6 m above the 9-m tall cottonwood canopy	

were made to the EC measurements: the krypton hygrometer ultraviolet beam was corrected for oxygen absorption using the relationship in Campbell Scientific (1989), and for varying air density using corrections in Webb et al. (1980). A Fourier series (Salas et al., 1980) was fitted to the ET measurements by Harrington et al. (2003) in order to extrapolate through periods of missing data, especially during wintertime when the equipment was removed for servicing and recalibration. The water year annual values applied in this paper were calculated and presented in Harrington et al. (2003).

Precipitation was measured either on the sites or at nearby USWB stations and the values used here are adopted from those reported by Harrington et al. (2003). ET_0 was calculated from the suite of data collected for estimation of ET within each of three regions of micrometeorologic measurements using methods presented in Allen et al. (1998). Missing wintertime data were filled using ratios of ET_0 from the measurement sites versus ET_0 calculated from daily California Irrigation Management System data collected in Bishop, California (California Department of Water Resources, CIMIS, undated) and also evaluated using methods described in Allen et al. (1998). The Bishop CIMIS site is located from 4 to 55 km from the sites where ET was measured.

San Luis Valley, Colorado

ET data collection is described in Cooper et al. (2004) and in Cooper et al. (2006). Sites were chosen for homogeneous cover with sufficient fetch distances, ca. 150–200 m in all directions. Each site was outfitted with groundwater monitoring wells and with Radiation Energy Balance Systems, (see Fritschen and Simpson, 1989) for measuring actual ET using the Bowen Ratio energy balance method (Tanner, 1960; Moncrief et al., 2000). The equipment that was used is described in Table 3 and in greater detail in Cooper et al. (2006). Daily ET_a calculated for the growing season at Moffat, Rito Alto and Thicket sites were combined with ET_a measured during the winter at Crestone to arrive at annual total ET_a for each site. During wintertime, ET_a of all sites essentially goes to a minimum value that represents soil surface evaporation (Cooper et al., 2004).

Precipitation was measured at each site with a tipping bucket rain gage. ET_0 was calculated from data measured at the Center, Colorado, CoAgMet station (Colorado State University, CoAgMet, undated) using methods in Allen et al. (1998). Center, Colorado is located between 27 and 50 km from the San Luis Valley ET measurement sites.

Bosque del Apache, New Mexico

The equipment and methods used for measuring cottonwood at one site and saltcedar at two sites are described in Bawazir (2000). ET_a measurements established for that study were continued at the same sites and with the same methods and equipment in a program funded by the State of New Mexico Interstate Stream Commission who provided the data for this analysis with permission for publication (Nabil Shafike, NMISC, personal communication, 2005). The primary ET method used was one propeller eddy covariance system (OPEC), with backup by three-dimensional EC

and additional measurements to close the energy balance. Bawazir (2000) found that the OPEC system was robust, reliable and, though comparatively inexpensive, provided data that were of the same quality as EC.

Not all annual data collected at the three study sites were used in this evaluation. Two years (WY 2000 and 2001) of data collected at the cottonwood site (SCWT) were excluded from consideration because of flooding during the summer of 2000. This caused large but transient evaporative fluxes that violated two of the assumptions for this method: lack of environmental homeostasis and surface water, or capillary-derived soil–surface evaporation.

ET_0 was calculated using data collected at the North Bosque weather station (New Mexico State University, undated) using methods from Allen et al. (1998). The North Bosque station is within several km of the three ET measurement sites. Minor missing portions of the ET record were filled with averages of ET data from the other years for each site (with the exclusion of SCWT data for WY2000 and 2001).

Precipitation measured at Bosque del Apache was used except for the period from September through December, 2001 due to a number of unusually high values (totaling 7× average annual precipitation for these four months) representing a spike that was absent in regional weather data (New Mexico State University, undated). These four months were replaced with data from Socorro, New Mexico, about 30 km to the north. Approximately 2.5 months of North Bosque precipitation data missing from the file for 2002 were filled with average data from the other three years.

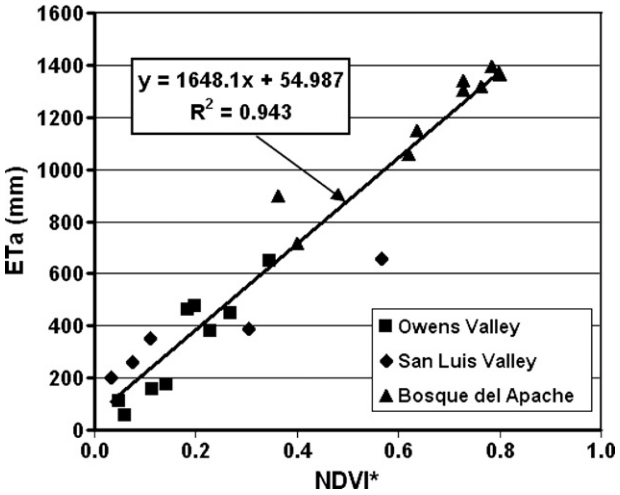

Figure 2 Annual ETa versus mid-summer NDVI*.

Results and discussion

NDVI data are presented in Table 2, and ET-related data in Table 4. The ET_a, pooled from all three studies, shows

Table 4 Annual water year total ET measured at four locations and 15 sites (total $n = 24$)

	Year	ET_a (mm)	FAO56 reference ET_0 (mm)	Precip. (mm)	ETa/ET_0	ET*
Owens Valley, California (Harrington et al., 2003)						
BLK100	2000	460	2021	35.6	0.2276	*0.2138*
BLK100	2001	449	1927	71.1	0.2330	*0.2037*
BLK009	2001	474	1927	71.1	0.2460	*0.2171*
PLC045	2001	156	1686	105.9	0.0925	*0.0317*
BLK100	2002	377	2012	32.5	0.1874	*0.1740*
FSL138	2002	646	1626	21.8	0.3973	*0.3891*
PLC018	2002	53	1885	34.5	0.0281	*0.0100*
PLC074	2002	175	1885	34.5	0.0928	*0.0759*
PLC185	2002	108	1885	34.5	0.0573	*0.0397*
San Luis Valley, Colorado Cooper et al. (2004)						
Standard	2000	200	1150	111.0	0.1739	*0.0857*
Crestone	2002	350	1135	106.9	0.3084	*0.2365*
Moffat	2002	261	1135	84.0	0.2303	*0.1688*
Rito Alto	2002	657	1135	87.3	0.5792	*0.5442*
Thicket	2002	386	1135	105.8	0.3401	*0.2723*
Bosque del Apache New Mexico (Bawazir, 2000, NMISC, 2005)						
SSCT	1999	1318	1775	159.3	0.7423	*0.7169*
NSCT	1999	1305	1775	159.3	0.7351	*0.7090*
SCWT	1999	898	1775	159.3	0.5062	*0.4575*
SSCT	2000	1373	1811	134.9	0.7582	*0.7388*
NSCT	2000	1397	1811	134.9	0.7713	*0.7529*
SSCT	2001	1362	1679	172.5	0.8113	*0.7897*
NSCT	2001	1340	1679	172.5	0.7983	*0.7752*
SSCT	2002	1150	1736	188.0	0.6627	*0.6217*
NSCT	2002	1059	1736	188.0	0.6099	*0.5625*
SCWT	2002	714	1736	188.0	0.4115	*0.3401*

strong linearity when graphed against NDVI* (Fig. 2). Thus, for these environments, NDVI* is a competent variable for predicting and mapping ET. This is an encouraging result considering the wide difference in ecology, leaf structure and canopy expression of the vegetation from the three combined studies. Vegetation canopies vary from 9-m tall cottonwood (SCWT), 6-m tall saltcedar (NSCT and SSCT in the Bosque del Apache), 0.3-m grass canopies in the shallow groundwater meadow (Rito Alto in the San Luis Valley) and scrub vegetation of various mixes of grasses and shrubs varying from 0.2 m to 1.5 m (sites in San Luis Valley and Owens Valley, about 1,100 km apart). The leaf structure of the dominant species was also highly varied from ca. 1 mm-long scales of saltcedar, to ca. 10-cm wide flat leaves of cottonwood, with ranges in-between.

Although climates of all three regions where ET was measured are arid, there are significant differences in climate type and seasonal expression. Both the San Luis Valley and Bosque del Apache are strongly influenced by the same summer Monsoonal weather pattern. However, the San Luis Valley experiences a much shorter growing season and much colder winters due to its elevation, at about 2400 m, and its location almost four degrees latitude north of Bosque del Apache. The Bosque del Apache is significantly lower at less than 1400 m elevation. The Owens Valley, at about 1200 m elevation, is strongly influenced by a Mediterranean type climate that seldom experiences summer precipitation. As these factors affect ET_a, the large differences in evaporative driving force of these climates needs to be factored into these calculations: this can be done using ET_0 that expresses vaporative driving force. The lowest annual total ET_0, calculated for San Luis Valley in 2002 was only 63% of the greatest annual total ET_0 calculated for Bosque del Apache in 2000 (Table 4).

The next to last column of Table 4 presents ET_a normalized by ET_0 (ET_a/ET_0), that is graphed against NDVI* in Fig. 3. The relationship in Fig. 3 does not pass through the origin, having a positively displaced *y*-intercept. Thus, for application in mapping ET_a, this *X*—*Y* relationship still requires calibration of NDVI* against spatially defined ET_a data sets such as those used for this comparison. As mentioned in the introduction, however, such data sets are very expensive, and seldom available *a priori*. What is needed is a more robust means of ET data portrayal for calibration of NDVI* to yield spatial values of ET_a.

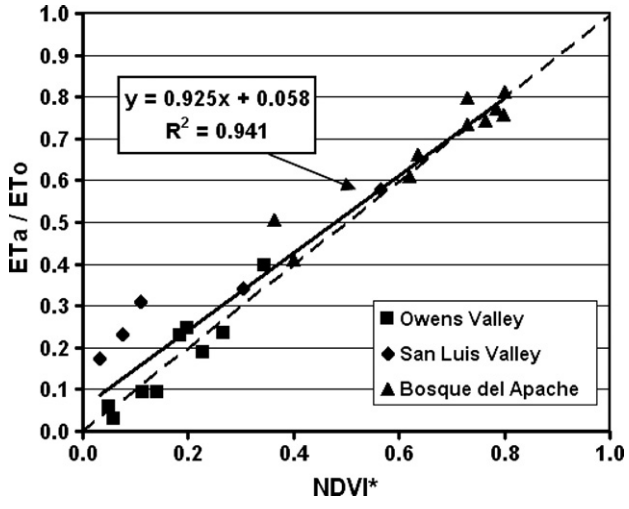

Figure 3 Annual ET_a/ET_0 versus mid-summer NDVI*. The regression line was calculated with all data ($n = 24$). For comparison, a one-to-one line is shown as a dash.

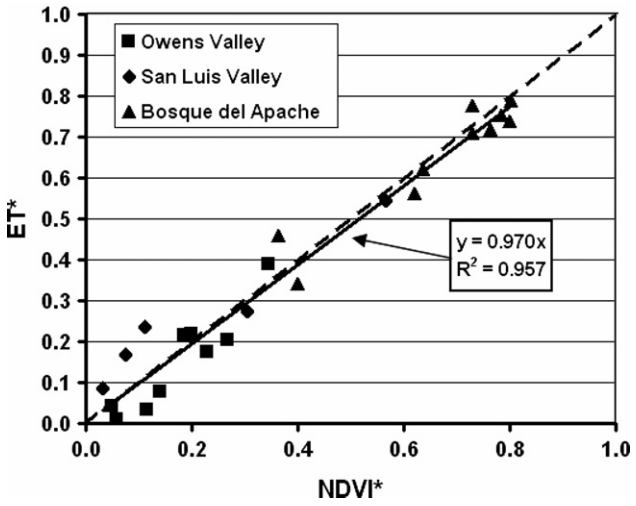

Figure 4 Annual ET* versus mid-summer NDVI*. The regression line was calculated with all data ($n = 24$). A one-to-one line is shown as a dash.

ET*, calculated using Eq. (2) as an annual total, is graphed against NDVI* (Fig. 4). To enable estimation procedures using this relationship, the regression line was forced through the origin with the resulting slope close to unity (0.970). This 1:1 approximation enables using NDVI* as a surrogate for ET*. Substituting NDVI* for ET* in Eq. (2) and rearranging then permitted estimation of ET_a, decoded with annual totals for ET_0 and precipitation according to Eq. (3).

$$ET_a(\text{estimated}) = (ET_0 - \text{Annual Precipitation})NDVI^* + \text{Annual Precipitation} \quad (3)$$

Minus the addition of the component of annual precipitation, Eq. (3) yields an estimate of groundwater discharge, ET_g, that is often of direct interest for groundwater modeling.

To evaluate the error that would arise using Eq. (3) for estimating annual total ET_a for the 24 site/year combinations, ET_a predicted from the single mid-summer point-in-time values of NDVI* were compared to measured ET_a (Table 5). Residual error showed that although individual estimation errors may be high (the largest being 151.5 mm/year) the combined errors tended to cancel one another in averages for the three study areas. Overall average errors for each of the three regions were relatively small — the largest being underprediction of about 45 mm/year for the average of all San Luis Valley sites that is an average underprediction of annual ET_a of about 12%.

A plot of the residual error as a percentage of measured ET_a is presented in Fig. 5. Residual errors were relatively well balanced and the magnitude of error strongly decreased as measured values of ET_a increased. This is an encouraging result because the method was most accurate at the highest levels of ET_a, and comparatively less so at low levels of ET_a.

Table 5 Measured ET_a compared to ET_a estimated from NDVI* using Eq. (3)

Site	Year	NDVI*	ET0 (mm)	Pptn. (mm)	Predicted ET_a	ET_a (mm)	Residual error	
							(mm/year)	% of ET_a
Owens Valley, California (Harrington et al., 2003)								
BLK100	2000	0.1859	2021	35.6	404.7	460.0	−55.3	−12.0
BLK100	2001	0.2686	1927	71.1	569.6	449.0	120.6	26.9
BLK009	2001	0.1995	1927	71.1	441.3	474.0	−32.7	−6.9
PLC045	2001	0.1151	1686	105.9	287.8	156.0	131.8	84.5
BLK100	2002	0.2286	1686	32.5	410.5	377.0	33.5	8.9
FSL138	2002	0.3462	1626	21.8	577.2	646.0	−68.8	−10.6
PLC018	2002	0.0601	1885	34.5	145.8	53.0	92.8	175.1
PLC074	2002	0.1420	1885	34.5	297.3	175.0	122.3	69.9
PLC185	2002	0.0497	1885	34.5	126.4	108.0	18.4	17.1
Average values					362.3	322.0	40.3	12.5
San Luis Valley, Colorado (Cooper et al., 2004)								
Standard	2000	0.0326	1150	111	144.9	200.0	−55.1	−27.5
Crestone	2002	0.1103	1135	106.9	220.3	350.0	−129.7	−37.1
Moffat	2002	0.0761	1135	84	164.0	261.4	−97.4	−37.3
Rito Alto	2002	0.5661	1135	87.3	680.4	657.4	22.9	3.5
Thicket	2002	0.3050	1135	105.8	419.7	386.0	33.7	8.7
Average values					325.9	371.0	−45.1	−12.2
Bosque del Apache New Mexico (Bawazir, 2000, NMISC, 2005)								
SSCT	1999	0.7634	1775	159.3	1392.7	1317.6	75.1	5.7
NSCT	1999	0.7289	1775	159.3	1336.9	1304.8	32.1	2.5
SCWT	1999	0.3637	1775	159.3	747.0	898.4	−151.5	−16.9
SSCT	2000	0.7993	1811	134.9	1474.6	1373.1	101.5	7.4
NSCT	2000	0.7846	1811	134.9	1450.0	1396.8	53.2	3.8
SSCT	2001	0.8016	1679	172.5	1380.0	1362.1	17.9	1.3
NSCT	2001	0.7292	1679	172.5	1271.1	1340.3	−69.3	−5.2
SSCT	2002	0.6365	1736	188.0	1173.3	1150.4	22.8	2.0
NSCT	2002	0.6204	1736	188.0	1148.4	1058.8	89.6	8.5
SCWT	2002	0.4001	1736	188.0	807.3	714.4	92.9	13.0
Average values					1218.1	1191.7	26.4	2.2

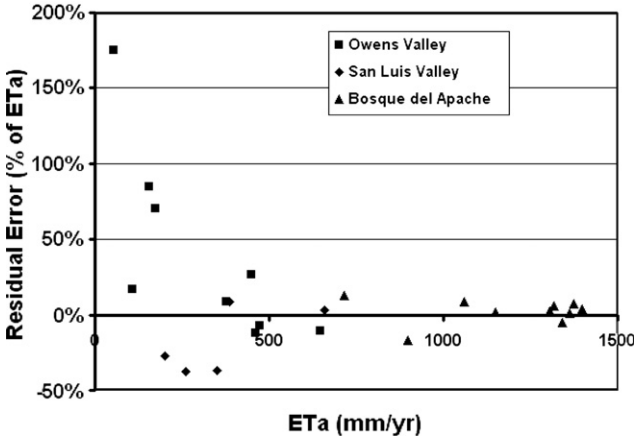

Figure 5 Residual error for annual ET_a predicted by Eq. (3) from mid-summer NDVI*.

One of the enabling assumptions for this method is that the canopy, as detectable using satellite-derived NDVI*, is the major influence moderating ET. The fact that higher levels of scatter occur at the lower end of ET_a may be an indication that other forms of water disposition such as canopy interception and soil evaporation of precipitation may be playing a role in determining whether the water becomes available for plant use and would, therefore, be detectable in canopy expression. Although this may be operating at some level, the simple mathematics of the transformation of ET_a to ET*, subtracting precipitation, will necessarily induce higher levels of scatter at the lower end of measured annual water use approaching the level of the annual precipitation. As ET_a approaches zero, projection of precipitation values measured elsewhere to a site as was performed for some of these comparisons can be expected to be a significant source of error. Even so, in conclusion, the errors do not appear to create a systematic bias. Therefore, the overall average water use estimates should be spatially correct, especially if used as a first-order estimation.

Sources of error for estimation of annual ET_a from the one-to-one relationship represented in Fig. 5 included unevaluated measurement and calculation errors for ET_0 and ET_a made in the three ET studies, and the potential

weather-related differences between the measurement sites and the stations that were used for calculating annual total ET_0 (up to 50 km distant) and precipitation (up to 30 km distant). When expressed as percent error, scatter was greatest at the lower end of the ET distribution, precisely where discrepancies between the values used for ET_0 and precipitation should have the greatest numerical impact.

An additional source of error for estimation of ET_a using NDVI* that affects all sites in this analysis are possible mismatches between the wind-induced fetch affects for the ET_a measurements and the NDVI data extracted to represent it — pixels were simply extracted in 3×3 matrices from around the geographic point of the micrometeorologic stations, and their NDVI values averaged. Even though attempts were made in each study to choose relatively homogeneous sites, examination of the NDVI values from the matrices indicated that inhomogeneity in vegetation vigor existed around most of the measurement sites. Thus, for more careful analyses, wind direction/magnitude should be included to identify the source region for correctly scaling the comparisons. In summary, much of the apparent error for the relationship (Figs. 4 and 5) may simply be due to scaling.

One of the outliers from the relationship in Fig. 5 is the SCWT data for 1999. Though this site was the subject of known flood irrigation in 2000 (and accordingly removed from consideration for 2000 and 2001), insufficient information existed to remove it from the data set during 1999 and so it remains in the data set as an outlier. The degree of scatter in these relationships should be viewed as a cautionary indication that (i) functional knowledge of the hydrology within the area of interest is important for application of the techniques described here, (ii) any mapping of ET_a can only be as accurate as the representation primarily of ET_0, and secondarily of precipitation, and (iii) for application, this method is intended for environments that share five characteristics:

- They are vegetated (plants moderate soil water loss);
- They are underlain by shallow groundwater (therefore, annual changes in ET are buffered by groundwater and ET peaks in mid-growing season);
- They have water tables generally remaining deeper than the limit for capillary rise (minimal or no surface evaporation from groundwater);
- They have an arid to semi-arid climate (emphasizing moderation by plants and the driving force of the atmosphere, ET_0);
- They are evaluated within a relative state of homeostasis (conditions remain the same leading up to and after the point-in-time snapshot provided by mid-summer satellite images).

Fortunately, all five of these ideal characteristics are often met over the majority of arid and semi-arid groundwater basins where water balance and ET are of interest. A dry climate ensures that the potential evaporation is far greater than precipitation. Here, vegetation that is afforded an extra water supply is greener (such as exists in riparian and shallow groundwater habitats) and readily contrasts with background vegetation of low greenery in surrounding upland habitats supported only by precipitation. An added benefit of ET estimation in dry climates using these techniques is the potential abundance of cloud-free satellite data.

In addition to providing for higher levels of canopy expression, the presence of shallow groundwater provides a buffer for water availability to ensure that peak canopy expression occurs in mid-summer. Stable water table position enhances this homeostasis, however, gradually changing water tables would conceivably not be a significant influence on the accuracy for ET estimation if the annual water use for the vegetation is relatively low compared to the water retained in the soil following water table decline. Such retained soil water may maintain sufficient annual supply and moderate the affects of watertable decline (Sorenson et al., 1991).

An example of an environment that would violate the requirements listed above would be where the water table approaches the surface sufficiently to enable surface evaporation by capillarity, and thus over time, salination and exclusion of plants. At least in the American west, the authors have identified this condition very rarely, and generally found it to be associated with restricted areas of groundwater seepage at the edge of playas. Additionally, salination is a process that takes place over decades to centuries and should not affect the estimates based upon an annual snapshot. Finally, there are simple and robust remote sensing techniques that can identify these sites by their surface wetness using Band 5 included in the same TM datasets that were used to derive these estimates (Lunetta and Balough, 1999; Frazier and Page, 2000). Even if such surface-discharge zones are dry during mid-summer, in the author's experience, they can be identified by telltale whitening by surface salts.

Conclusion

When applied to single mid-summer scenes, the ET estimation algorithm provides annual total ET_a based on the mid-summer canopy expression within each 28.5 m pixel (approximately 0.2 acre). This algorithm requires multi-band satellite data, and a series of processing steps that:

1. Correct for atmospheric scatter (dark object subtraction),
2. Calculate NDVI,
3. Convert NDVI to NDVI* using scene-derived statistics.

As a first-order approximation for mapping annual ET, the method can be applied to any environment supported by shallow groundwater where sufficient weather data are available for calculation of annual values of precipitation and ET_0.

The algorithm is intended for spatial mapping of ET over large arid-to-semi-arid groundwater basins and requires environments in which vegetation provides the dominant moderation for ET. Thus, the ideal environment is underlain by shallow groundwater, is vegetated, relatively homeostatic, e.g., absent transient surface flooding that would greatly increase evaporation, and lacks capillary rise from the water table to the soil surface (that would enhance

the evaporation component while leaving NDVI unaffected). Fortunately, many groundwater basins of the arid-semi-arid American West are dominated by these conditions. Where surface wetting by overland flow or capillary rise from shallow groundwater violate the ideal conditions and induce higher ET rates, these effects can be mapped using other simple and robust techniques that conveniently use another band of the same Landsat TM data (Lunetta and Balough, 1999). Thus identified, the ET_a of these lands could be quantified as some fraction of ET_0 to improve the first-order estimates of ET_a for the basin.

Acknowledgements

The authors thank the Board of the Rio Grande Water Conservation District for its support in development of this technique and writing this paper and especially Ralph Curtis, David Robbins and Allen Davey for their interest and insights. We thank Dr. Bob Harrington of the Inyo County Water Department for graciously supplying the Owens Valley data set, Dr. Nabil Shafike of the New Mexico Interstate Stream Commission for the ET data set measured at Bosque del Apache, Dr. A.S. Bawazir of New Mexico State University, for the data set from North Bosque and Dr. Rick Allen for advance review and insightful comments.

References

Allen, R.B., Pereira, L.S., Raes, D., Smith, M.S., 1998. Crop evapotranspiration (guidelines for computing crop water requirements). FAO irrigation and drainage paper 56. 300pp.

Arya, S.P., 2001. Introduction to Micrometeorology, second ed. Academic Press.

Baugh, W.M., Groeneveld, D.P., 2006. Broadband vegetation index performance evaluated for a low-cover environment. International Journal of Remote Sensing 27, 4715—4730.

Bawazir, A.S., 2000. Saltcedar and Cottonwood Riparian Evapotranspiration of the Middle Rio Grande. Ph.D. Dissertation, Department of Civil Engineering, New Mexico State University.

Buschmann, C., Nagel, E., 1993. In vivo spectroscopy and internal optics of leaves as basis for remote sensing of vegetation. International Journal of Remote Sensing 14, 711—722.

California Department of Water Resources, CIMIS. undated. Bishop, California weather data. <http://wwwcimis.water.ca.gov/cimis/welcome.jsp> (Accessed August, 2005).

Campbell Scientific, Inc. 1989. KH2 Krypton Hygrometer. Revision 11/89.

Chong, D.L.S., Mougin, E., Gastellu-Etchegorry, J.P., 1993. Relating the global vegetation index to net primary productivity and actual evapotranspiration over Africa. International Journal of Remote Sensing 14, 1517—1546.

Colorado State University. CoAgMet. undated. Center, Colorado weather data. <http://ccc.atmos.colostate.edu/~coagmet/> (Accessed August 2005).

Cooper, D.J., .Sanderson, J, Groeneveld, D.P., Chimner, R.A., 2004. Evapotranspiration rates for non-wetland phreatophyte communities — 1996—2002. Unpublished report prepared for the Rio Grande Water Conservation District. 67pp.

Cooper, D.J., Sanderson, J.S., Stannard, D.I., Groeneveld, D.P., 2006. Effects of water table drawdown on evapotranspiration, vegetation composition and leaf area in an arid region phreatophyte community. Journal of Hydrology 325, 21—34.

Curran, P.J., Dungan, J.L., Gholz, H.L., 1992. Seasonal LAI in slash pine estimated with Lansat TM. Remote Sensing of the Environment 39, 3—13.

Frazier, P.S., Page, K.J., 2000. Water body detection and delineation with Landsat TM data. Photogrammetric Engineering & Remote Sensing 66, 1461—1467.

Fritschen, L.J., Simpson, J.R., 1989. Surface energy and radiation balance systems: general descriptions and improvements. Journal of Applied Meteorology 28, 680—689.

Gash, J.H.C., 1986. A note on estimating the effect of a limited fetch on micrometerological evaporation measurements. Boundary Layer Meterology 35, 409—413.

Gillies, R.R., Carlson, T.N., Cui, J., Kustas, W.O., Humes, K.S., 1997. A verification of the 'triangle' method for obtaining surface soil water content and energy fluxes from remote measurements of the normalized difference vegetation index (NDVI) and surface radiant temperature. International Journal of Remote Sensing 18, 3145—3166.

Grist, J., Nicholoson, S.E., Mpolokan, A., 1997. On the use of NDVI for estimating rainfall fields in the Kalahari of Botswana. Journal of Arid Environments 35, 195—214.

Groeneveld, D.P., Baugh, W.M., 2007. Correcting satellite data to detect vegetation signal for eco-hydrologic analyses. Journal of Hydrology, doi:10.1016/j.jhydrol.2007.07.001.

Harrington, R., Steinwand, A., Hubbard, P.J., Martin, D., Stroh, J., Or, D., 2003. Evapotranspiration from groundwater dependent plant communities: comparison of micrometeorological and vegetation-based measurements. Draft Cooperative Study Progress Report prepared by the County of Inyo Water Department and Los Angeles Department of Water and Power. 79pp. and appendices.

Hobbs, T.J., 1995. The use of NOAA-AVHRR NDVI data to assess herbage production in the arid rangelands of Central Australia. International Journal of Remote Sensing 16, 1289—1302.

Huete, A.R., Liu, H.Q., 1994. An error and sensitivity analysis of the atmospheric- and soil-correcting variants of the NDVI for the MODIS-EOS. IEEE Transactions on Geoscience and Remote Sensing 32, 897—905.

Irish, R., 1999. Landsat 7 Science Data Users Handbook. <http://ltpwww.gsfc.nasa.gov/IAS/handbook.html>, Landsat Project Science Office, Goddard Space Flight Center (last accessed April 2007).

Kerr, Y.H., Imbernon, J., Dedieu, G., Hautecoeur, O., Lagouarde, J.P., Seguin, B., 1989. NOAA AVHRR and its uses for rainfall and evapotranspiration monitoring. International Journal of Remote Sensing 10, 847—854.

Kustas, W.P., Perry, E.M., Doraiswamy, P.C., Moran, M.S., 1994. Using satellite remote sensing to extrapolate evapotransiration estimates in time and space over a semiarid rangeland basin. Remote Sensing of Environment 49, 275—286.

Liu, H.Q., Huete, A.R., 1995. A feedback based modification of the NDVI to minimize canopy background and atmospheric noise. IEEE Transactions on Geoscience and Remote Sensing 33, 457—465.

Lunetta, R.S., Balough, M.E., 1999. Application of multi-temporal Landsat 5 TM imagery for wetland identification. Photogrammetric Engineering & Remote Sensing 65, 1303—1310.

Meinzer, O.E., 1927. Plants as indicators of groundwater. US Geological Survey Water Supply Paper 577. 95pp.

Moncrief, J., Jarvis, P., Valentini, R., 2000. Canopy fluxes. In: Sala, O.E., Jackson, R.B., Mooney, H.A. (Eds.), Methods in Ecosystem Science. Springer-Verlag, New York, pp. 161—180.

New Mexico State University, undated. North Bosque del Apache, New Mexico weather data. <http://weather.nmsu.edu/cgi-shl/cns/stninfo.pl?stn=21> (Accessed December 2005).

Nichols, W.D., 2000. Regional ground-water evapotranspiration and ground-water budgets, Great Basin, Nevada. US Geological Survey Professional Paper 1628. 82pp.

Nichols, W.D., Laczniak, R.J., DeMeo, G.A., Rapp, T.R., 1997. Estimated ground-water discharge by evapotranspiration, Ash Meadows area, Nye County, Nevada, 1994: US Geological Survey Water Resources Investigation Report 97-4025, 13pp.

Or, D., Groeneveld, D.P., 1994. Stochastic estimation of plant-available soil water under fluctuating water table depths. Journal of Hydrology 163, 43—64.

Paruelo, J.M., Epstein, H.E., Lauenroth, W.K., Burke, I.C., 1997. ANPP estimates from NDVI for the central grassland region of the Untied States. Ecology 78, 953—958.

Rouse, J.W., Haas, R.H., Schell, J.A., Deering, D.W., 1974. Monitoring vegetation systems in the great plains with ERTS. In: Proceedings Third ERTS Symposium, NASA SP-351, 10—14 December 1973, Washington, DC, NASA Scientific and Technical Information Office, Washington pp. 309—317.

Salas, J.D., Delleur, W., Yevjevich, V., Lane, W.L., 1980. Applied modeling of hydrologic time series. Water Resource Publications, Fort Collins, Colorado. 498pp.

Seevers, P.M., Ottmann, R.W., 1994. Evapotranspiration estimation using a normalized difference vegetation index transformation of satellite data. Hydrological Sciences Journal 39, 333—345.

Sellers, P.J., Berry, J.A., Collatz, G.J., Field, C.B., Hall, F.G., 1992. Canopy reflectance, photosynthesis and transpiration. III. A reanalysis using improved leaf models and a new canopy integration scheme. International Journal of Remote Sensing 42, 187—216.

Sorenson, S.K., Dileanis, P.D., Branson, F.A., 1991. Soil water and vegetation responses to precipitation and changes in depth to ground water in Owens Valley, California. US Geological Survey Water-Supply Paper 2370G. 36pp.

Szilagyi, J., 2002. Vegetation indices to aid areal evapotranspiration estimations. Journal of Hydrologic Engineering 7, 368—372.

Szilagyi, J., 2000. Can a vegetation index derived from remote sensing be indicative of areal transpiration? Ecological Modeling 127, 65—79.

Szilagyi, J., Parlange, M.B., Rundquist, D.C., Gosselin, D.C., 1998. NDVI relationship to monthly evaporation. Geophysical Research Letters 25, 1753—1756.

Tanner, C.B., 1960. Energy balance approach to evapotranspiration from crops. Soil Science Society of America Proceedings 24, 1—9.

Tucker, C.J., Sellers, P.J., 1986. Satellite remote sensing of primary production. International Journal of Remote Sensing 7, 1395—1416.

Webb, E., Pearman, G.I., Leuning, R., 1980. Correction of flux measurements for density effects due to heat and water vapor transfer. Quarterly Journal of the Research Meteorological Society 106, 85—100.